Modeling of dynamic and spectral viscoelastic characteristics of composite materials

A. Valishin[1*] and *M.* Tinyaev[1]

[1]Bauman Moscow State Technical University, 2nd Baymanskaya Str., 105005, Moscow, Russia

Abstract. When designing products made of composite materials intended for use in difficult conditions of inhomogeneous deformations and temperatures, it is important to take into account viscoelastic, including spectral and dynamic, properties of the binder and fillers. The article considers dynamic characteristics (complex modulus, complex malleability, their real and imaginary parts, loss angle tangent) and spectral characteristics of relaxation and creep and their dependence on each other. The above-mentioned characteristics were found for all known types of creep kernel and relaxation kernel. To find the spectral characteristics, one of the numerical methods of reversing the Laplace transformation was used - the method of quadrature formulas. Algorithms and computer programs have been compiled to implement this method. Key words: composite materials, viscoelastic properties, spectral properties, dynamic properties, Laplace transformation, quadrature formulas.

1 Introduction

When designing products made of composite materials intended for use in difficult conditions of inhomogeneous deformations and temperatures, it is important to take into account the viscoelastic properties of the binder and fillers [1]. All viscoelastic characteristics, both static and dynamic, are expressed, ultimately, through relaxation and creep nuclei [2, 17].

Relaxation and creep kernel reflect the specific properties of a particular material. There are many model variants of such cores proposed at different times scattered in the literature. All of them were systematized and brought together in the work [17], and a mutual connection between them was established there [17]. An alternative and generalized approach is to determine the spectral characteristics of relaxation and creep - the density of the relaxation spectrum and the creep spectrum. It is necessary to link all the defining viscoelastic functions through spectral characteristics. It is also necessary to establish the relationship between the relaxation spectral density and the creep spectral density.

Thus, the density of relaxation spectra, for example, becomes the primary and main viscoelastic characteristic of the material, it is specific to each specific material and is subject to experimental determination in each specific case. In this work, a partial implementation of this program is proposed.

* Corresponding author: enf@mail.ru

2 Mathematical formulations of the problem, accepted assumptions

For isotropic viscoelastic materials, the defining relations between stress and strain tensors are written as follows

$$\sigma(t)=G(t)\varepsilon(0)+\int_0^t G(t-\tau)\frac{\partial\varepsilon(\tau)}{\partial\tau}d\tau,\ \varepsilon(t)=J(t)\sigma(0)+\int_0^t J(t-\tau)\frac{\partial\sigma(\tau)}{\partial\tau}d\tau, \qquad (1)$$

Where $G(t)$ and $J(t)$ are relaxation and creep functions, respectively [1-15].

The function $G(t)$ describes the change in stress over time with constant deformation. This process is called stress relaxation. In this process, the tension decreases with time, that is, the function $G(t)$ is decreasing.

The function $J(t)$ describes the change in deformation over time at constant stress. This process is called creep deformation. In the process of creep at constant stress, the deformation increases, that is, the function $J(t)$ is increasing.

In the theory of elasticity between an elastic module G and malleability J there is a simple connection [1-4]

$$GJ=1. \qquad (2)$$

However, in the theory of viscoelasticity, there is no such simple connection between the relaxation and creep functions.

Let's write down formulas (1) in the Laplace image space using the convolution theorem

$$\overline{\sigma}(p)=p\overline{G}(p)\overline{\varepsilon}(p),\quad \overline{\varepsilon}(p)=p\overline{J}(p)\overline{\sigma}(p). \qquad (3)$$

From formulas (3) follows

$$p^2\overline{G}(p)\overline{J}(p)=1. \qquad (4)$$

This expression defines the relationship between the images of relaxation and creep functions.

In the theory of the Laplace transform, the following limiting relations take place

$$\lim_{t\to 0+}G(t)J(t)=1,\quad \lim_{t\to+\infty}G(t)J(t)=1, \qquad (5)$$

That is, relations of type (2) in the theory of viscoelasticity take place only in two limiting cases: when $t\to 0+$ and when $t\to+\infty$.

Convenient relaxation function $G(t)$ and creep function $J(t)$ present in dimensionless form.

To do this, we denote

$$G(t)=G_0\psi(t),\ \ G(0)=G_0,\ [Pa];\ \ J(t)=J_0 g(t),\ \ J(0)=J_0,\ [Pa^{-1}]. \tag{6}$$

The functions $\psi(t)$ and $g(t)$ are dimensionless. The function $\psi(t)$ is called the relaxation kernel, and the function $g(t)$ is the creep kernel.

By virtue of (2) and (5) it will be

$$G_0 J_0=1,\quad \lim_{t\to 0+}\psi(t)g(t)=1,\quad \lim_{t\to+\infty}\psi(t)g(t)=1. \tag{7}$$

In the Laplace image space between the images of dimensionless functions $\psi(t)$ and $g(t)$ there is a relation of type (4):

$$p^2\overline{\psi}(p)\overline{g}(p)=1. \tag{8}$$

3 Dynamic characteristics of viscoelastic materials and the relationship between them

The most well-known dynamic characteristics are the complex module $G^*(i\omega)$ and the complex malleability $J^*(i\omega)$:

$$G^*(i\omega)=i\omega G_0\tilde{\psi}(\omega),\ J^*(i\omega)=i\omega J_0\tilde{g}(\omega), \tag{9}$$

Where $\tilde{\psi}(\omega)$ and $\tilde{g}(\omega)$ are the images of the relaxation kernel and the creep kernel, respectively, in the Fourier space.

There is the following relationship between formulas (9) [14-16]:

$$G^*(i\omega)J^*(i\omega)=1. \tag{10}$$

Complex modulus and complex malleability, as the name implies, have real and imaginary parts:

$$G^*(i\omega)=G'(\omega)+iG''(\omega),\ \ J^*(i\omega)=J'(\omega)+iJ''(\omega), \tag{11}$$

Where $G'(\omega)$ and $G''(\omega)$ are real (accumulation modulus) and imaginary (loss modulus) parts of complex module, $[Pa]$; $J'(\omega)$ and $J''(\omega)$ are real and imaginary parts of complex compliance, $\left[Pa^{-1}\right]$.

By substituting formulas (11) into (10) we obtain the following expressions

$$G'(\omega)J'(\omega)-G''(\omega)J''(\omega)=1,\ \ G'(\omega)J''(\omega)+G''(\omega)J'(\omega)=0, \tag{12}$$

from which important ratios can be obtained:

$$\begin{aligned} G'(\omega) &= J'(\omega)\left|J^*(i\omega)\right|^{-2}, \quad G''(\omega) = -J''(\omega)\left|J^*(i\omega)\right|^{-2}, \\ J'(\omega) &= G'(\omega)\left|G^*(i\omega)\right|^{-2}, \quad J''(\omega) = -G''(\omega)\left|G^*(i\omega)\right|^{-2}. \end{aligned} \tag{13}$$

Let's return to expressions (12) and write the second equation in the form

$$G''(\omega)\left[G'(\omega)\right]^{-1} = -J''(\omega)\left[J'(\omega)\right]^{-1}, \tag{14}$$

Where the left side of the equality, by definition, is called the tangent of the loss angle $tg\alpha$, so

$$tg\alpha = G''(\omega)\left[G'(\omega)\right]^{-1}. \tag{15}$$

Then it follows from (14) and (15) that

$$tg\alpha = -J''(\omega)\left[J'(\omega)\right]^{-1}. \tag{16}$$

4 Relaxation and creep spectra and their relation to relaxation and creep kernels

In [2-3], the relaxation function $G(t)$ is defined as follows:

$$G(t) = \int_0^{+\infty} H(\tau)\exp\left[-t\tau^{-1}\right]d\tau + G_\infty, \tag{17}$$

Where $H(\tau)$ is the relaxation time distribution function (relaxation spectrum), $\left[Pa \cdot s^{-1}\right]$.

Taking into account (6), the relaxation kernel $\psi(t)$ is expressed in terms of the relaxation spectrum $H(\tau)$ as

$$\psi(t) = (G_0)^{-1}\left\{\int_0^{+\infty} H(\tau)\exp\left[-t\tau^{-1}\right]d\tau + G_\infty\right\}. \tag{18}$$

From this formula by substitution $\tau \to \gamma^{-1}$ we can get the expression

$$\int_0^{+\infty} \gamma^{-2} H\left(\gamma^{-1}\right) \exp\left[-t\gamma\right] d\gamma = G_0 \psi\left(t\right) - G_\infty, \tag{19}$$

in which the integral expression is nothing but a direct Laplace transform. This means that the function $\gamma^{-2} H\left(\gamma^{-1}\right)$ is the original, and the function $G_0 \psi\left(t\right) - G_\infty$ is the image. By inverting the Laplace transform, we can define $\gamma^{-2} H\left(\gamma^{-1}\right)$ by $\psi\left(t\right)$, and then by reverse substitution $\gamma \to \tau^{-1}$ we find $H\left(\tau\right)$:

$$H\left(\tau\right) = \tau^{-2}\left[G_0 \mathrm{L}^{-1}\left\{\psi\left(t\right)\right\} - G_\infty \delta\left(\tau^{-1}\right)\right], \tag{20}$$

Where L^{-1} is the inverse Laplace transform operator; $\delta\left(\tau^{-1}\right)$ is the Dirac delta function, $\left[s\right]$. Since the value G_∞ is a constant, the summand $\tau^{-2} G_\infty \delta\left(\tau^{-1}\right)$ at $0 < \tau < +\infty$ is zero. Then (20) takes a simpler form:

$$H\left(\tau\right) = G_0 \tau^{-2} \mathrm{L}^{-1}\left\{\psi\left(t\right)\right\}. \tag{21}$$

In [2-3], the creep function $J\left(t\right)$ is defined as

$$J\left(t\right) = \int_0^{+\infty} j\left(\tau\right)\left\{1 - \exp\left[-t\tau^{-1}\right]\right\} d\tau + J_0, \tag{22}$$

Where $j\left(\tau\right)$ is the lag time distribution function, or creep spectrum, $\left[Pa^{-1} \cdot s^{-1}\right]$.

Taking into account (6), the creep kernel $g\left(t\right)$ is expressed in terms of the creep spectrum $j\left(\tau\right)$ as

$$g\left(t\right) = 1 + \left(J_0\right)^{-1} \int_0^{+\infty} j\left(\tau\right)\left\{1 - \exp\left[-t\tau^{-1}\right]\right\} d\tau. \tag{23}$$

By substitution $\tau \to \gamma^{-1}$ we obtain an expression similar to (20), applying to which the inverse of the Laplace transform, we define $j\left(\tau\right)$:

$$j\left(\tau\right) = \tau^{-2}\left[J_\infty \delta\left(\tau^{-1}\right) - J_0 \mathrm{L}^{-1}\left\{g\left(t\right)\right\}\right], \tag{24}$$

Where $J_\infty = J\left(t\right)\big|_{t \to +\infty} = \int_0^{+\infty} j\left(\tau\right) d\tau + J_0$.

Note that the summand $\tau^{-2}J_{\infty}\delta\left(\tau^{-1}\right)$ at $0<\tau<+\infty$ is zero, if $J_{\infty}=const\neq 0$ (a viscoelastic solid). Then (24) is written in the form $j\left(\tau\right)=-J_0\tau^{-2}\mathrm{L}^{-1}\left\{g\left(t\right)\right\}$. For the case when $J_{\infty}=+\infty$ (viscous or viscoelastic fluid), the summand $\tau^{-2}J_{\infty}\delta\left(\tau^{-1}\right)$ is undefined.

5 Relation of relaxation and creep spectra to each other

According to (8), there is a mutual relationship between the relaxation kernel $\psi\left(t\right)$ and the creep kernel $g\left(t\right)$ in the Laplace image space. Taking into account (18) and (23), it becomes obvious that the functions of the relaxation spectrum $H\left(\tau\right)$ and the creep spectrum $j\left(\tau\right)$ are also not independent.

Let's define formulas linking the spectra together. Let's start with the fact that from (18) we find the image of the relaxation kernel. Then, using (8), we find the image of the creep kernel. Applying the inverse Laplace transform operator L^{-1} to the function $J_{\infty}p^{-1}-J_0\overline{g}\left(p\right)$, we get an expression similar to (20) from which we can get the function $\gamma^{-2}j\left(\gamma^{-1}\right)$. By reverse substitution $\gamma\to\tau^{-1}$ we find the creep spectrum $j\left(\tau\right)$, and then, taking into account (5) and (7), the final formula takes the form

$$j\left(\tau\right)=\tau^{-2}\left[\left(G_{\infty}\right)^{-1}\delta\left(\tau^{-1}\right)-\mathrm{L}^{-2}\left\{\left[p^2\mathrm{L}^2\left\{\gamma^{-2}H\left(\gamma^{-1}\right)\right\}+G_{\infty}p\right]^{-1}\right\}\right], \qquad (25)$$

Where L^2 and L^{-2} are operators of direct and inverse Laplace transformations, respectively, applied twice.

Similarly, we can derive a formula expressing the relaxation spectrum through the creep spectrum:

$$H\left(\tau\right)=\tau^{-2}\mathrm{L}^{-2}\left\{\left[J_{\infty}p-p^2\mathrm{L}^2\left\{\gamma^{-2}j\left(\gamma^{-1}\right)\right\}\right]^{-1}\right\}. \qquad (26)$$

6 Known types of relaxation and creep functions

In [17], the known types of relaxation and creep kernels and their derivatives (Abel, Rabonov, Rzhanitsyn functions, etc.) were presented in the form of tables. Using these data, the dynamic and spectral characteristics of each of these kernels were further found.

6.1 Dynamic and Spectral Characteristics of Creep and Relaxation Kernels

Using the data from the tables from [17] and the formula (9)-(16), (21) and (24) the dynamic and spectral characteristics of the known creep kernels and relaxation kernels were obtained. The results are shown in Tables 1-6.

Maxwell functions

Table 1 shows the dynamic and spectral characteristics of Maxwell kernels.

Table 1. Dynamic and spectral characteristics of Maxwell kernels.

№	Relaxation	Creep
1	$\exp\left[-\tau^{-1}t\right]$	$1+\tau^{-1}t$
2	$G_0 t^{-2}\delta\left(t^{-1}-\tau^{-1}\right)$	$J_0 t^{-2}\left(\tau^{-1}t-1\right)\delta\left(t^{-1}\right)$
3	$G_0 i\tau\omega\left(1+i\tau\omega\right)^{-1}$	$J_0\left(1-i\tau^{-1}\omega^{-1}\right)$
4	$G_0\tau^2\omega^2\left(1+\tau^2\omega^2\right)^{-1}$	J_0
5	$G_0\tau\omega\left(1+\tau^2\omega^2\right)^{-1}$	$-J_0\tau^{-1}\omega^{-1}$
6	$\tau^{-1}\omega^{-1}$ $+\infty$	0

Kohlrausch functions

Table 2 shows the dynamic and spectral characteristics of Kohlrausch kernels.

Table 2. Dynamic and spectral characteristics of Kohlrausch kernels.

№	Relaxation	Creep
1	$\exp\left[-\tau^{\beta-1}t^{1-\beta}\right]$ $\sum_{r=0}^{+\infty}(-1)^r\left(r!\right)^{-1}\tau^{z(-r)}t^{z(r)}$	$\sum_{r=0}^{+\infty}b_r\left\{\Gamma\left[1+z(r)\right]\right\}^{-1}\tau^{z(-r)}t^{z(r)}$
2	$G_0 t^{-2}\sum_{r=0}^{+\infty}(-1)^r\left\{r!\Gamma\left[z(-r)\right]\right\}^{-1}\tau^{z(-r)}t^{z(r)+1}$	$J_0 t^{-2}\sum_{r=0}^{+\infty}b_r\left\{s\left[z(r)\right]\right\}^{-1}\tau^{z(-r)}t^{z(r)+1}$
3	$G_0\sum_{r=0}^{+\infty}(-1)^r\Gamma\left[1+z(r)\right]\left[r!(\tau\omega)^{z(r)}\right]^{-1}\exp\left[-0.5i\pi z(r)\right]$	$J_0\sum_{r=0}^{+\infty}b_r(\tau\omega)^{z(-r)}\exp\left[-0.5i\pi z(r)\right]$
4	$G_0\sum_{r=0}^{+\infty}(-1)^r\Gamma\left[1+z(r)\right]\left[r!(\tau\omega)^{z(r)}\right]^{-1}\cos\left[0.5\pi z(r)\right]$	$J_0\sum_{r=0}^{+\infty}b_r(\tau\omega)^{z(-r)}\cos\left[0.5\pi z(r)\right]$
5	$G_0\sum_{r=0}^{+\infty}(-1)^{r+1}\Gamma\left[1+z(r)\right]\left[r!(\tau\omega)^{z(r)}\right]^{-1}\sin\left[0.5\pi z(r)\right]$	$-J_0\sum_{r=0}^{+\infty}b_r(\tau\omega)^{z(-r)}\sin\left[0.5\pi z(r)\right]$

In Table 2 β takes values $0\le\beta\le 1$, $b_0=1$,

$b_r=\sum_{k=1}^{r}(-1)^{k-1}\left[(k-1)!\right]^{-1}\Gamma\left[z(k)\right]b_{r-k}$, $r=1,2,...,+\infty$, $z(k)=k(1-\beta)$,

$z(r)=r(1-\beta)$, $s\left[z(r)\right]=\pi\left\{\sin\left[\pi z(r)\right]\right\}^{-1}$. When $\beta=0$, Kohlrausch's characteristics turn into Maxwell's characteristics.

Abel functions

Table 3 shows the dynamic and spectral characteristics of Abel kernels.

Table 3. Dynamic and spectral characteristics of Abel kernels.

№	Relaxation	Creep
1	$\sum_{r=0}^{+\infty}\left[-\Gamma(\beta)\right]^r\left[\Gamma(1-z)\right]^{-1}\tau^z t^{-z}$	$1+\beta^{-1}\tau^{-\beta}t^{\beta}$
2	$G_0 t^{-2}\sum_{r=0}^{+\infty}\left[-\Gamma(\beta)\right]^r\left[s(z)\right]^{-1}\tau^z t^{1-z}$	$-J_0 t^{-2}\left\{\delta\left(t^{-1}\right)+\beta^{-1}\left[\Gamma(-\beta)\right]^{-1}\tau^{-\beta}t^{\beta+1}\right\}$

3	$G_0\sum_{r=0}^{+\infty}\left[-\Gamma(\beta)\right]^r(\tau\omega)^z\exp[0.5i\pi z]$	$J_0\left\{1+\Gamma(\beta)(\tau\omega)^{-\beta}\exp[-0.5i\pi\beta]\right\}$	
4	$G_0\sum_{r=0}^{+\infty}\left[-\Gamma(\beta)\right]^r(\tau\omega)^z\cos[0.5\pi z]$	$J_0\left\{1+\Gamma(\beta)(\tau\omega)^{-\beta}\cos[0.5\pi\beta]\right\}$	
5	$G_0\sum_{r=0}^{+\infty}\left[-\Gamma(\beta)\right]^r(\tau\omega)^z\sin[0.5\pi z]$	$-J_0\Gamma(\beta)(\tau\omega)^{-\beta}\sin[0.5\pi\beta]$	
6	$\sin[0.5\pi\beta]\left\{(\tau\omega)^{\beta}\left[\Gamma(\beta)\right]^{-1}+\cos[0.5\pi\beta]\right\}^{-1}$	$tg[0.5\pi\beta]$	0

In Table 3 β takes values $0<\beta\le 1$, $s(z)=\pi\left[\sin(\pi z)\right]^{-1}$, $z=-r\beta$. When $\beta=1$, Abel's characteristics turn into Maxwell's characteristics.

7.4 Rabotnov functions

Table 4 shows the dynamic and spectral characteristics of the Rabotnov kernels.

Table 4. Dynamic and spectral characteristics of Rabotnov kernels.

№	Relaxation	Creep	
1	$1-\sum_{r=0}^{+\infty}(-1)^r\left[\Gamma(1-z_1)\right]^{-1}\tau^{z_1}t^{-z_1}$	$1+\left[\Gamma(1-z_2)\right]^{-1}\tau^{z_2}t^{-z_2}$	
2	$G_0t^{-2}\left\{\delta(t^{-1})-\sum_{r=0}^{+\infty}(-1)^r\left[s(z_1)\right]^{-1}\tau^{z_1}t^{1-z_1}\right\}$	$-J_0t^{-2}\left\{\delta(t^{-1})+\left[s(z_2)\right]^{-1}\tau^{z_2}t^{1-z_2}\right\}$	
3	$G_0\left\{1+\sum_{r=0}^{+\infty}(-1)^r(z_1)^{-1}(\tau\omega)^{z_1}\exp[0.5i\pi z_1]\right\}$	$J_0\left\{1+(\tau\omega)^{z_2}\exp[0.5i\pi z_2]\right\}$	
4	$G_0\left\{1+\sum_{r=0}^{+\infty}(-1)^r(z_1)^{-1}(\tau\omega)^{z_1}\cos[0.5\pi z_1]\right\}$	$J_0\left\{1+(\tau\omega)^{z_2}\cos[0.5\pi z_2]\right\}$	
5	$G_0\sum_{r=0}^{+\infty}(-1)^r(z_1)^{-1}(\tau\omega)^{z_1}\sin[0.5\pi z_1]$	$J_0(\tau\omega)^{z_2}\sin[0.5\pi z_2]$	
6	$-\sin[0.5\pi z_2]\left\{(\tau\omega)^{-z_2}+\cos[0.5\pi z_2]\right\}^{-1}$	$-tg[0.5\pi z_2]$	0

In Table 4 γ takes values $0<\gamma\le 1$, $s(z)=\pi\left[\sin(\pi z)\right]^{-1}$, $z_1=-\gamma(r+1)$, $z_2=-\gamma$. When $\gamma=1$, Rabotnov's characteristics turn into Maxwell's characteristics.

7.5 Rzhanitsyn functions

Table 5 shows the dynamic and spectral characteristics of the Rzhanitsyn kernels.

Table 5. Dynamic and spectral characteristics of Rzhanitsyn kernels.

№	**Relaxation**	**Creep**
1	$1-\gamma(z_1,\tau^{-1}t)\left[\Gamma(z_1)\right]^{-1}$	$1+\sum_{r=1}^{+\infty}\gamma(z_2,\tau^{-1}t)\left[\Gamma(z_2)\right]^{-1}$
2	$G_0t^{-2}\left[s(z_1)\right]^{-1}\theta(t)\left(\tau t^{-1}-1\right)^{-z_1}$	$J_0t^{-2}\left\{\theta(t)\sum_{r=1}^{+\infty}\left[s(z_2)\right]^{-1}\left(\tau t^{-1}-1\right)^{-z_2}-\delta(t^{-1})\right\}$
3	$G_0\left\{1-\left[\rho(\omega)\right]^{-z_1}\exp\left[-iz_1\varphi(\omega)\right]\right\}$	$J_0\left\{1+\sum_{r=1}^{+\infty}\left[\rho(\omega)\right]^{-z_2}\exp\left[-iz_2\varphi(\omega)\right]\right\}$

4	$G_0\left\{1-\left[\rho(\omega)\right]^{-z_1}\cos\left[z_1\varphi(\omega)\right]\right\}$	$J_0\left\{1+\sum_{r=1}^{+\infty}\left[\rho(\omega)\right]^{-z_2}\cos\left[z_2\varphi(\omega)\right]\right\}$		
5	$G_0\left[\rho(\omega)\right]^{-z_1}\sin\left[z_1\varphi(\omega)\right]$	$-J_0\sum_{r=1}^{+\infty}\left[\rho(\omega)\right]^{-z_2}\sin\left[z_2\varphi(\omega)\right]$		
6	$\sin\left[z_1\varphi(\omega)\right]\left\{\left[\rho(\omega)\right]^{z_1}-\cos\left[z_1\varphi(\omega)\right]\right\}^{-1}$		$+\infty$	0

In Table 5 β takes values $0<\beta\le 1$, $\theta(t)=th\left(\tau t^{-1}-1\right)$, $h\left(\tau t^{-1}-1\right)$ is the Heaviside function, $s(z)=\pi\left[\sin(\pi z)\right]^{-1}$, $z_1=\beta$, $z_2=r\beta$, $\gamma\left(\beta,\tau^{-1}t\right)=\int_0^{\tau^{-1}t}\xi^{\beta-1}\exp[-\xi]d\xi$ is the lower incomplete gamma function [18-19], $\varphi(\omega)=arctg(\tau\omega)$, $\rho(\omega)=\left(1+\tau^2\omega^2\right)^{1/2}$. When $\beta=1$, Rzhanitsyn's characteristics turn into Maxwell's characteristics.

Gavriljak-Negami functions

Table 6 shows the dynamic and spectral characteristics of Gavrilyak-Negami kernels.

Table 6. Dynamic and spectral characteristics of Gavrilyak-Negami kernels.

№	Relaxation	Creep
1	$1-\sum_{r=0}^{+\infty}(-1)^r a(r)\left[\Gamma(1-z_1)\right]^{-1}\tau^{z_1}t^{-z_1}$	$1+\sum_{r=1}^{+\infty}\sum_{m=0}^{+\infty}(-1)^m D_m\left[\Gamma(1-z_2)\right]^{-1}\tau^{z_2}t^{-z_2}$
2	$G_0t^{-2}\left\{\delta\left(t^{-1}\right)-\sum_{r=0}^{+\infty}(-1)^r a(r)\left[s(z_1)\right]^{-1}\tau^{z_1}t^{1-z_1}\right\}$	$-J_0t^{-2}\left\{\delta\left(t^{-1}\right)+\sum_{r=1}^{+\infty}\sum_{m=0}^{+\infty}(-1)^m D_m\left[s(z_2)\right]^{-1}\tau^{z_2}t^{1-z_2}\right\}$
3	$G_0\left\{1-\sum_{r=0}^{+\infty}(-1)^r a(r)(\tau\omega)^{z_1}\exp\left[0.5i\pi z_1\right]\right\}$	$J_0\left\{1+\sum_{r=1}^{+\infty}\sum_{m=0}^{+\infty}(-1)^m D_m(\tau\omega)^{z_2}\exp\left[0.5i\pi z_2\right]\right\}$
4	$G_0\left\{1-\sum_{r=0}^{+\infty}(-1)^r a(r)(\tau\omega)^{z_1}\cos\left[0.5\pi z_1\right]\right\}$	$J_0\left\{1+\sum_{r=1}^{+\infty}\sum_{m=0}^{+\infty}(-1)^m D_m(\tau\omega)^{z_2}\cos\left[0.5\pi z_2\right]\right\}$
5	$-G_0\sum_{r=0}^{+\infty}(-1)^r a(r)(\tau\omega)^{z_1}\sin\left[0.5\pi z_1\right]$	$J_0\sum_{r=1}^{+\infty}\sum_{m=0}^{+\infty}(-1)^m D_m(\tau\omega)^{z_2}\sin\left[0.5\pi z_2\right]$

In Table 6 α, β takes values $0<\alpha\le 1$, $0<\beta\le 1$, $z_1=-\alpha(r+\beta)$, $z_2=-\alpha(r\beta+m)$, $D_m=\sum_{k_1=0}^{m}\sum_{k_2=0}^{k_1}\cdots\cdots\sum_{k_{r-1}}^{k_{r-2}}\prod_{j=0}^{r-1}a\left(k_j-k_{j+1}\right)$,

$a(r)=\Gamma(r+\beta)\left[r!\Gamma(\beta)\right]^{-1}$, $k_0=m$, $k_r=0$, $r=1,2,...,+\infty, m=0,1,...,+\infty$, $s(z)=\pi\left[\sin(\pi z)\right]^{-1}$. When $\alpha=1$, Gavrilyak-Negami 's characteristics turn into Rzhanitsyn's characteristics, and when $\alpha=\beta=1$ they turn into Maxwell's characteristics.

In tables 1-6, the functions of the kernels are indicated under number 1, the spectra of the kernels are indicated under number 2, the complex module and complex compliance are indicated under number 3, respectively, and their real and imaginary parts are indicated under numbers 4-5. Number 6 indicates the tangent of the loss angle and its limit values at $\omega\to 0+$ and at $\omega\to+\infty$, respectively.

Remark. Using Tables 1-6 and (13), it is possible to obtain the following functions already in an analytical form: the Abel accumulation modulus and the Abel loss modulus, the Rabotnov accumulation modulus and the Rabotnov loss modulus, the real and imaginary parts of the complex malleability of Rzhanitsyn.

6.2 Numerical method for solving the problem

Relaxation and creep spectra, according to (21) and (24), are found through relaxation and creep kernels by reversing the Laplace transform. We will solve this problem using one of the numerical methods of reversing the Laplace transform - the method of quadrature formulas with equal coefficients [20]. This method was described in detail in the previous work [17].

6.3 Examples of numerical solution of the problem

Computer programs were written that implement the method of quadrature formulas for finding spectra. Here are some calculations obtained using these programs.

Figures 1-6 show graphs obtained by the method of quadrature formulas. To construct the functions of the spectra, the following parameters were set: $\tau = 100$ (for the Rabotnov spectra $\tau = 20$), β=0.5, γ=0.5, $h = 0.5$, $s = 1$, $G_0 = 1$, $J_0 = 1$.

Figures 1, 3 and 5 show graphs of the relaxation spectra of Abel, Rabotnov and Rzhanitsyn, respectively.

Figures 2, 4 and 4 show graphs of the creep spectrum of Abel, Rabotnov and Rzhanitsyn, respectively.

The green graphs correspond to the analytical functions (or in the form of an approximate finite series) of the spectra, while the red graphs correspond to the functions of the spectra obtained by the numerical method mentioned above.

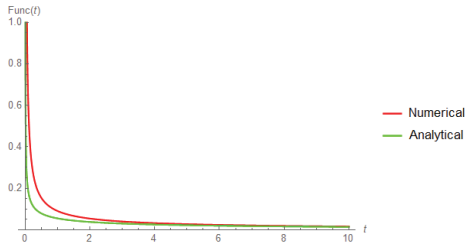

Fig. 1. Abel relaxation spectrum at $n = 100$, $\Delta H_{cp} \approx 0.05$.

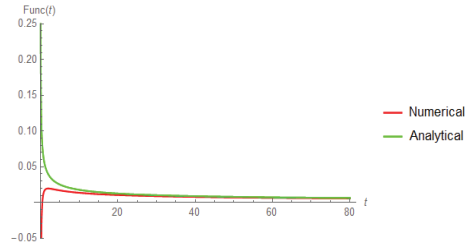

Fig. 2. Abel creep spectrum at $n = 100$, $\Delta j_{cp} \approx 0.008$.

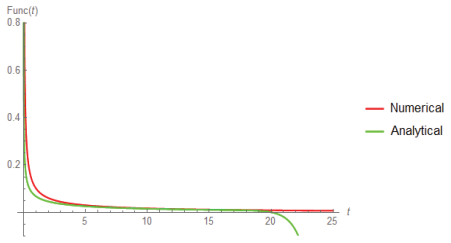

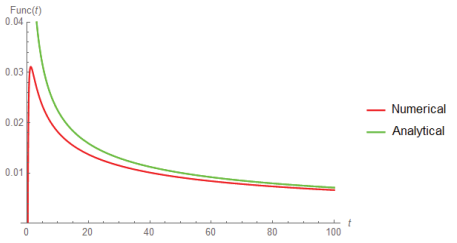

Fig. 3. Rabotnov relaxation spectrum at $n = 100$, $\Delta H_{cp} \approx 0.025$.

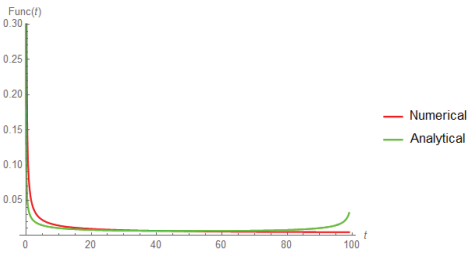

Fig. 4. Rabotnov creep spectrum at $n = 100$, $\Delta j_{cp} \approx 0.006$.

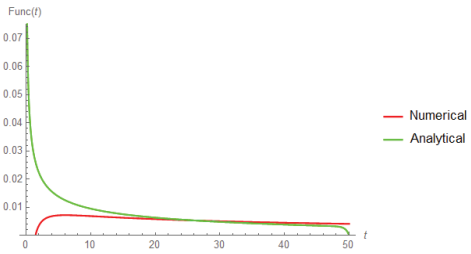

Fig. 5. Rzhanitsyn relaxation spectrum at $n = 100$, $\Delta H_{cp} \approx 0.007$.

Fig. 6. Rzhanitsyn creep spectrum at $n = 100$, $\Delta j_{cp} \approx 0.003$.

All the necessary calculations were performed in the Wolfram Mathematica.

7 Conclusions

After analyzing the results, we draw the following conclusions:

1) the graphs of the relaxation and creep spectra were obtained fairly accurately (the maximum error of calculations does not exceed 5% on average), despite the fact that the error is very noticeable in the initial time sections. Numerical finding of the functions of the Kohlrausch and Gavriljak-Negami yield spectra caused difficulties associated with a complex recursive formula in these kernels;

2) for all kernels (except for the kernels of Kohlrausch and Gavrilyak-Negami), their dynamic characteristics were obtained in the form of analytical functions, even though the functions of some kernels are represented as an approximate infinite series;

3) formulas defining the spectra through each other have not proved to be very effective in practice (with the exception of Maxwell spectra). It is possible that for greater efficiency, the direct and inverse Laplace transform in these formulas should be replaced by an approximate one (the integrand function should be written as an approximate infinite series).

References

1. YU.I. Dimitriyenko, *Nelineynaya mekhanika sploshnoy sredy* (FIZMATLIT, M., 2009)
2. R. Kristensen, *Vvedeniye v teoriyu vyazkouprugosti* (Izd-vo Mir., Moskva, 1974)
3. D. Blend, *Teoriya lineynoy vyazko-uprugosti* (Izd-vo Mir., Moskva, 1965)
4. I.A. Birger, YA.G. Panovko, *Prochnost', ustoychivost', kolebaniya - Spravochnik v trokh tomakh. T. 1. Pod red* (izdatel'stvo "Mashinostroyeniye", Moskva, 1968)
5. YU.I. Dimitriyenko, *Mekhanika sploshnoy sredy: uchebnoye posobiye: v 4-kh tomakh* (MGTU im. N.E. Baumana, Tom 4: Osnovy mekhaniki tvordykh sred, Moskva, 2013)
6. L.D. Landau, YE.M. Lifshits, *Teoreticheskaya fizika: Ucheb. posob.: dlya vuzov. V 10 t. T.VII. Teoriya uprugosti* (5-ye izd., stereot FIZMATLIT, M., 2003)
7. YU.N. Rabotnov, *Polzuchest' elementov konstruktsiy* (Nauka, M., 1966)
8. M.A. Koltunov, *Polzuchest' i relaksatsiya*, Izd-vo Vysshaya shkola (1976)
9. B.V. Moskvitin, *Soprotivleniye vyazkouprugikh materialov* (Nauka., M., 1972)

10. A.R. Rzhanitsyn, *Teoriya polzuchesti*, Izd-vo lit-ry po stroitel'stvu (1968)
11. G.M. Bartenev, S.YA. Frenkel', *Fizika polimerov* (Khimiya, L., 1990)
12. B.YE. Pobedrya, *Mekhanika kompozitsionnykh materialov* (Izd-vo Mosk. un-ta, M., 1984)
13. YU.I. Dimitriyenko, YU.V. Yurin, S.V. Sborshikov, A.D. Yakhnovskiy, R.R. Baymurzin, Matematicheskoye modelirovaniye i chislennyye metody **3**, 22–46 (2020)
14. YU.I. Dimitriyenko, YE.A. Gubareva, D.O. Yakovlev, Nauchnoye izdaniye MGTU im. N.E. Baumana **10**, 359–382 (2014)
15. YU.I. Dimitriyenko, YE.A. Gubareva, S.V. Sborshikov, Matematicheskoye modelirova-niye i chislennyye metody **2**, 28–48 (2014)
16. B.D. Coleman, Thermodynamics of Materials with Memory, Arch. Ratioc. Mech., Anal. **17**, 1 (1964)
17. D. Ferri, (IL, Vyazkouprugiye svoystva polimerov, 1963)
18. B. Gross, (Paris, Mathematical Structure of the Theories of Viscoelasticity, 1953)
19. A.A. Valishin, M.A. Tinyayev, Matematicheskoye modelirovaniye i chislennyye metody **3**, 3–21 (2020)
20. Y.E. Yanke, F. Emde, F. Lesh, *Spetsial'nyye funktsii* (Fizmatgiz, Moskva, 1968)
21. V.I. Pagurova, *Tablitsy nepolnoy gamma-funktsii* (Fizmatgiz. Moskva, 1963)
22. V.I. Krylov, N.S. Skoblya, *Metody priblizhonnogo preobrazovaniya Fur'ye i obrashcheniya preobrazova-niya Laplasa. Glavnaya redaktsiya fiziko-matematicheskoy literatury izdatel'stva* (Nauka, M., 1974)